Influence of Thickness of Screen Printed Carbon Electrodes on Electrochemical Sensing

Priyanka Ganguly, Deepan Kumar Neethipathi, Ajay Beniwal, Ravinder Dahiya*
Bendable Electronics and Sensing Technologies (BEST), Group, University of Glasgow, G12 8QQ, Glasgow, UK
*Correspondence to - Ravinder.Dahiya@glasgow.ac.uk

***Abstract*— Screen printing is one of the widely used methods for printed sensors and electronics. The performance of these devices could vary with the printing parameters such as thickness of the printed layer, the squeeze length and pressure applied for printing *etc.* Whilst sensor design and the ink used for the printing of sensitive layers have been studied previously, the vital printing parameters has not attracted much attention. This paper reports the influence of thickness of printed sensor on their electrochemical sensing property. Carbon ink is used to print sensors with three-electrode geometry and their working electrode is modified with MoS_2 to study the detection of ascorbic acid. The thicknesses of the sensitive layers varied from ~4 μm to 120 μm as the number of printed layers of ink increased from 1 to 5, 10 and 20. The cyclic voltammetry, differential pulse voltammetry and impedance spectroscopy are used to investigate the electrochemical performance. It was noted that the peak current indicating the oxidation of ascorbic acid at 0.04 V, increased with the increase in the thickness of electrode or the number of printed layers. The higher current values and lower series resistance was measured for layers 10 and 20, indicating the ideal printed thickness of sensors for low power operation and easy interfacing with read out electronics.**

Keywords—Screen printing; printed sensor; electrochemistry; ascorbic acid; Electrochemical Sensors, Flexible Electronics

I. Introduction

Screen printing (SP) is a popularly used method for development of various types of low-cost sensors (*e.g.* gas, physical, and chemical sensors) and electronics as it provides resource efficient manufacturing route [1-4]. The mechanical, electrical, and optical properties of screen-printed sensors are known to be influenced by the electrode parameters such as geometrical design, roughness, and the material [5-7]. Along with these, the thickness of the printed electrode hugely impacts the characteristics like flexibility, photoluminescence *etc*. [8, 9]. In the case of electrochemical sensor, a thick film is required to imitate their macro equivalent performance and a stable potential (reference electrode) for good electrode - electrolyte interaction [10, 11]. This is also needed in electrochemical sensing as the thin film electrodes can easily worn off due to gradual degradation of electrode material, cracks formation and fouling or corrosion [12, 13]. Moreover, thinner layer suffers less signal to noise ratio compared to the thicker layered SP electrodes. Therefore, multi-layered coated screen-printed sensors are needed for reliable function.

Generally, the thickness of the SP sensor can be varied through several parameters such as ink property (*e.g.*, viscosity, adhesion); printing parameters (*e.g.*, squeegee pressure; distance between the substrate and the stencil); stencil parameters (*e.g.*, mesh gap and number of meshes) *etc*. [14, 15]. An alternative method is layer by layer deposition of electrodes until the thickness leading to optimal response is achieved. Whilst thick film sensors have been studied in literature the layer-by-layer printing to obtain desired thickness has not attracted much attention. In this work, we present the electrochemical sensor performance of screen-printed carbon electrode (SPCE) by varying their thickness *via* increasing the number of printed layers. Here, the optimization of thickness for SPCE based electrochemical sensor is discussed through impedance and electrochemical measurements; to further understand the electrode-electrolyte interaction of the printed electrodes and finally, a resultant of high signal to noise ratio is achieved. Carbon ink is used to print sensors with three-electrode geometry and their working electrode is modified with MoS_2 to study the detection of ascorbic acid.

This paper is organised as follows: The materials and methods used for the development of sensors are given in Section II. The results from evaluation of humidity sensors are given in Section III and the key outcomes are explained in Section IV.

II. Materials and Methods

A. Materials

Sodium molybdate and thiourea were purchased from Merck. Commercial carbon ink (conductive) for screen printing the electrodes was purchased from Sun chemicals. Ascorbic acid, Phosphate Buffer Saline (PBS) tablets and Dimethylformamide (DMF), isopropyl alcohol (IPA) were purchased from Merck. The chemicals obtained are used without any further purification.

B. Synthesis of MoS_2

The precursor mixture of thiourea and sodium molybdate was used to prepare the Molybdenum disulfide (MoS_2) using hydrothermal synthesis route. For this, 6.24 g (0.080 moles) of thiourea was mixed in 60 mL of deionized (DI) water along with 4.84 g (0.020 moles) of sodium molybdate. The mixture was kept for stirring for 1 hr at room temperature. As prepared mixture was further transferred into stainless steel autoclave (100 mL Teflon lined, from Parr instruments), which was kept at 220 ºC inside the oven for 24 hrs followed by cooling to room temperature conditions. The precipitated black powder obtained inside the autoclave vessel is transferred into centrifuge tube (50 mL) and washed several times with DI water and isopropyl alcohol. As obtained precipitated black powder is dried at 60 ºC inside a heating oven for 12 hrs. Furthermore, the as prepared MoS_2 nanomaterial is dissolved in DMF (at 20 mg/mL concentration) and utilized for

This work was supported in part by the Engineering and Physical Sciences Research Council through Engineering Fellowship for Growth (EP/R029644/1) and European Commission through Innovative Training Network AQUASENSE (H2020-MSCA-ITN-2018-813680).

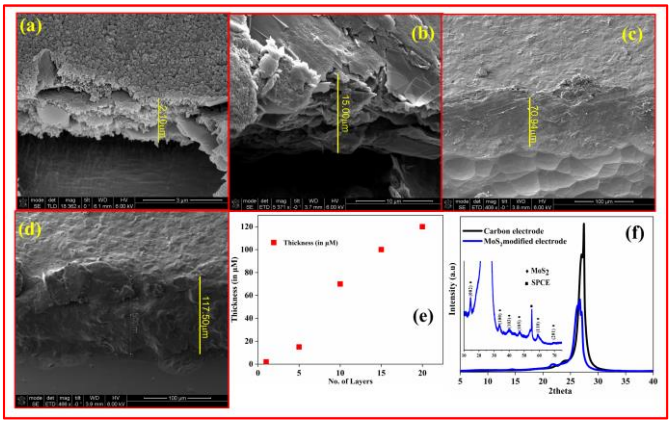

Fig. 1 SEM images of screen-printed carbon electrode (a) layer 1; (b) layer 5; (c) layer 10; (d) layer 20 and (e) Plot of the number of layers *vs* thickness and (d) XRD of carbon electrode and modified electrode.

modifying the working electrode (WE) of the screen-printed sensors.

C. Screen printing and Characteriztions

Three electrode system having working electrode (WE) with a diameter of 10 mm, reference electrode (RE) and counter electrode (CE) has been screen printed using carbon ink on the flexible polyvinyl chloride (PVC) substrate using screen printer (*Aurel Automation Stencil Printer C920)*). The electrode system was printed in different configuration as 1, 5, 10 and 20 layered. The squeeze pressure and length used was 1.8 Kg and 16 cm respectively. The distance between the screen and the squeeze (print gap) was maintained at 2 mm. For multiple layer configuration, the layers were screen printed followed by drying process at RT. As printed electrodes are cured at 70 ºC for 1 hr. Further, to develop the connection points, the wiring was realised using the same carbon ink followed by placing small amount of dielectric ink. Using the drop casting method, 30 µL of MoS_2 (20 mg/mL) solution in DMF was used to modify the working electrode followed by annealing at 65 ºC for 30 minutes. The electrochemical properties of the printed sensors were examined using CV, DPV and EIS analysis, which were carried out using the Metrohm Autolab (PGSTAT302N). The X-ray diffraction was carried out using XRD P'Analytical X'Pert with Cu Kα (λ = 1.541 Å). While SEM images were taken by FEI Nova.

III. Results and Discussion

A. Material characterisation

The printed sensors at different layer (*n* =1, 5, 10 and 20) were further characterized by SEM to evaluate the thickness of the printed electrodes. Fig. 1 (a-d) displays the SEM images of printed electrodes at different magnifications, with their thickness measured. The thickness varies from about 4 µm to 120 µm. A plot comparing the thickness to the number of printed layers displays almost a linear relationship (Fig. 1(e)). The maximum printed layers are twenty, as beyond that point the interspacing gap between the electrodes and track width start to reduce, which would alter the electrode geometry. The printed electrodes of varying thickness were further modified with MoS_2 to evaluate the influence of thickness to the electrochemical sensing. The diffractogram of the carbon electrode and the modified electrode (*n*=20) is displayed in Fig. 1(f). The peaks of carbon at ~27.3º corresponds to its

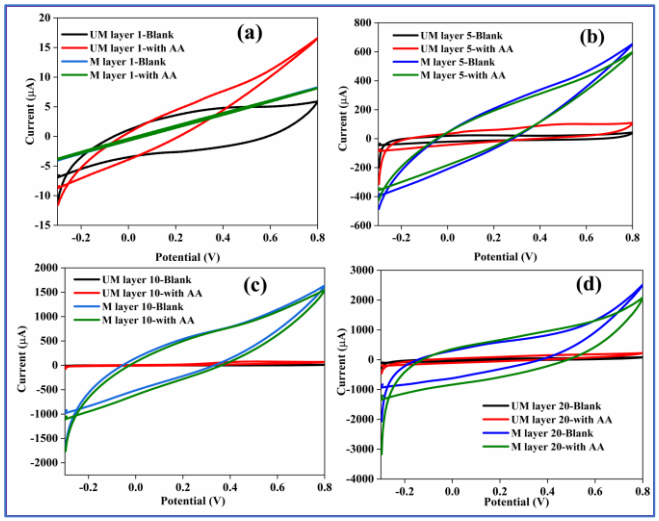

Fig. 2. CV profile of unmodified and modified sensors in presence and absence of 100 µM AA at a scan rate of 50 mV/s. (a) layer 1; (b) layer 5; (c) layer 10; and (d) layer 20.

(002) plane [16]. While the modified electrode displays the peak of both MoS_2 and carbon [17]. The inset of the figure provides more information about the identifiable peaks. The peaks of MoS_2 correspond to the hexagonal (2H) structure and do not display any further impurity [16] [17].

B. Electrochemical sensing analysis

The printed sensors at different layer (*n* =1, 5, 10 and 20), with and without modification of the working electrode were utilised for comparatively assessment. Ascorbic acid was chosen as an analyte to detect using the varied layers of modified (M layer *n*) and unmodified sensors (UM layer *n*). The cyclic voltammograms of the unmodified and modified sensors in presence and absence of 100 µM AA, at a scan rate of 50 mV/s for a potential window of -0.3 V to 0.8 V is displayed in Fig. 2. The single layer sensor displays a very small current in the micron range. Moreover, the modified electrode does not display any improvement to the sensing or sensitivity (Fig. 2(a)). The modification of the electrodes with MoS_2 is evident by the change in the CV pattern observed. The rectangular profile for the unmodified electrode turned into

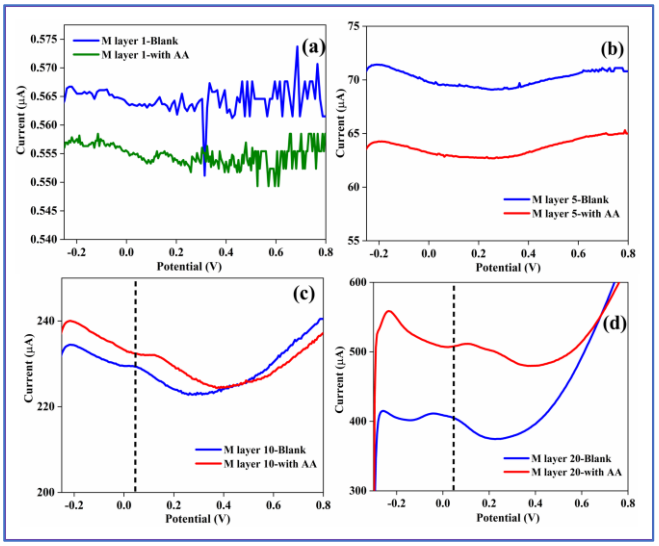

Fig. 3. DPV profiles of modified sensors in presence and absence of 100 µM AA at a scan rate of 50 mV/s. (a) layer 1; (b) layer 5; (c) layer 10; and (d) layer 20.

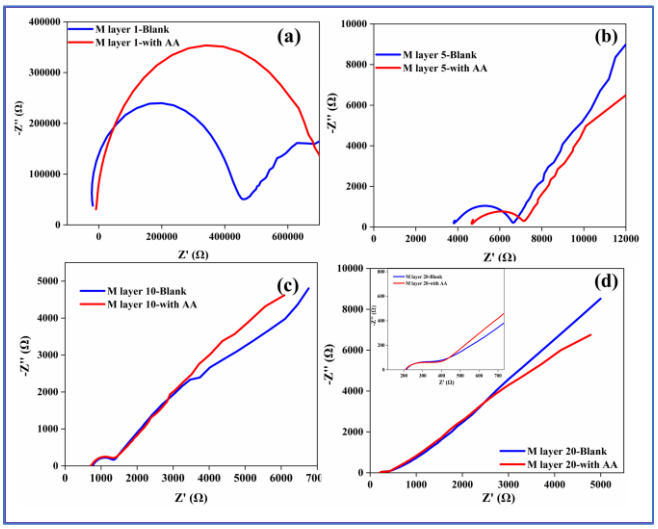

Fig. 4. Nyquist plot of modified sensors in presence and absence of 100 μM AA (a) layer 1; (b) layer 5; (c) layer 10; and (d) layer 20.

pseudo-rectangular shape. Increasing the layer value to five, improves the measured current for both the modified and unmodified electrodes. However, the presence of AA was still not evident in the peak potentials (Fig. 2(b)). The increased layer thickness values to ten and twenty, resulted in increased current, almost up to 6 folds (Fig. 2 (c) and (d)). The oxidation peak of AA is observed at 0.044 V and similarly a reduction peak is also observed around (-0.1 V) [18, 19]. Similarly, the DPV profiles of varied layers of modified (M layer *n*) in presence and absence of 100 μM AA is displayed in Fig. 3. Single layered sensor with modification displayed noisy DPV curves as shown in Fig. 3(a). The current value measured increased as the thickness improved to five layers. However, the overall sensitivity towards the electrochemical sensing of AA was not observed (Fig. 3(b)). This is similar to the results observed in their respective CV profile. While the DPV profile of thicker sensors (n =10, 20) display similar attributes to the CV. The peak current increased as well as displayed slight shift in the peak on addition of AA, as indicated in Fig. 3(c and d). The shift in the peak confirms the detection process.

To understand the charge transfer characteristics of the printed sensors of varying thickness, the electrochemical impedance spectroscopy (EIS) measurements were also carried out. EIS was performed from 1 MHz to 0.01 Hz. The impedance response (Nyquist plot) of the modified sensors in presence and absence of 100 μM AA is displayed in Fig. 4. The real and the imaginary value of impedance is plotted across the X and Y axes, respectively. The single layer printed electrode (Fig. 4 (a)) displayed a big semicircle at higher

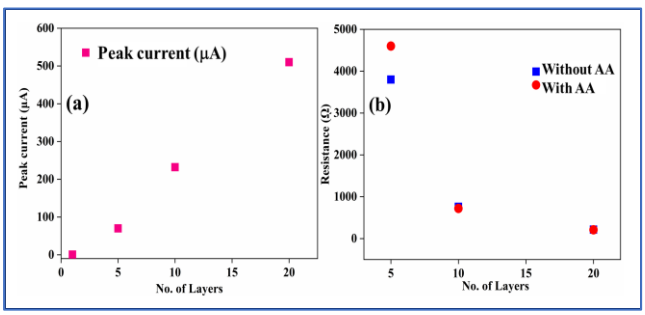

Fig. 5. (a) Peak current *vs* number of layers and (b) Series resistance measured for modified sensors in presence and absence of 100 μM AA.

TABLE I. SUMMARISED VALUE OF SERIES RESISTANCE (R_S) MEASURED FOR MODIFIED DIFFERENT SENSORS

Printed Layer (n)	Series resistance (R_s) in Ω	
	Without Analyte	*With Analyte*
5	3811	4665
10	746	713
20	214	210

frequency and a smaller one at lower frequency. The first semicircle is attributed to the bulk electrolyte resistance observed and the latter one is as a result of the electrode resistance [20]. However, on addition of the analyte, the diameter of the first semicircle enlarged and the electrode resistance was not observed [21]. Increasing the printed layers decreased the overall equivalent series resistance measured for the different sensors. The complex phase plot observed for the rest of all the sensors (n = 5, 10 and 20) is basically divided into three distinct segments: (1) high frequency zone where the semicircles are formed; (2) the medium frequency zone where details about charge transport and ion diffusion is observed; and, (3) low frequency zone where a linear line parallel to the Y-axis provides understandings about the internal capacitance developed (Fig. 4 (b-d)) [22]. The semicircle observed for these modified electrodes at high frequency region, could be attributed to the electric double layer formation due to the modification on the working electrode by MoS_2. Finally, a Warburg impedance is introduced in the low frequency region, characteristic to the diffusion process. In all the plots, addition of the analyte resulted in a slight change to the series resistance (R_s). Table 1 tabulates the series resistance measured for the different sensors in presence and absence of AA.

The electrochemical detection provides a clear inference towards the influence of layer thickness on the sensing ability. Fig. 5 provides plots detailing the peak current measured and the series resistance (R_s) for 100 μM AA detection at 0.044 V for different printed layers. For a singular layer printed sensor displayed extremely noisy and low current values along with high electrode and electrolyte resistance. The increase in the printed layer improved the current measured and subsequently decreased the resistance values as observed in Fig. 5 (b). The lower current values measured could not be utilised for remote monitoring, as the signal strength is quite low. Based on these results, the ideal number of layers to be printed are between 10 and 20.

IV. CONCLUSION

In summary, the present work demonstrates the influence of printing thickness on electrochemical sensing. The printed layer displayed varying range of thickness as observed in the SEM images. The modification of the working electrode with MoS_2 allowed us to understand the influence of thickness in the sensing ability. The low current value and high resistance measured for lower thickness-based sensors demonstrates the influence of thickness of the printed electrodes for the detection process. The higher current values are registered for layers 15 and 20, which would be ideal for interfacing with commercial read out electronics which requires low power. The outcomes from study show that number of printing layers could be another new factor for tuning the output of printed electrochemical sensors and will add new dimension in terms of their design flexibility.

References

[1] C. Wang, K. Xia, H. Wang, X. Liang, Z. Yin, and Y. Zhang, "Advanced carbon for flexible and wearable electronics," *Advanced materials*, vol. 31, no. 9, p. 1801072, 2019.

[2] S. Dervin, P. Ganguly, and R. Dahiya, "Disposable electrochemical sensor using Graphene oxide–chitosan modified carbon-based electrodes for the detection of tyrosine," *IEEE Sensors Journal*, vol 21 (23), pp 26226 - 26233, 2021.

[3] F. Nikbakhtnasrabadi, S. E. Hosseini, S. Dervin, D. Shakthivel, and R. Dahiya, "Smart Bandage with Inductor-Capacitor Resonant Tank based Printed Wireless Pressure Sensor on Electrospun Poly-L-lactide nanofibers," *Advanced Electronic Materials*, 2022, doi: 10.1002/aelm.202101348.

[4] M. Bhattacharjee, F. Nikbakhtnasrabadi, and R. Dahiya, "Printed chipless antenna as flexible temperature sensor," *IEEE Internet of Things Journal*, vol. 8, no. 6, pp. 5101-5110, 2021.

[5] R. R. Suresh *et al.*, "Fabrication of screen-printed electrodes: opportunities and challenges," *Journal of Materials Science*, vol. 56, no. 15, pp. 8951-9006, 2021.

[6] D. E. Riemer, "The theoretical fundamentals of the screen printing process," *Microelectronics International*, 1989.

[7] S. Khan, W. Dang, L. Lorenzelli, and R. Dahiya, "Flexible pressure sensors based on screen-printed P (VDF-TrFE) and P (VDF-TrFE)/MWCNTs," *IEEE Transactions on Semiconductor Manufacturing*, vol. 28, no. 4, pp. 486-493, 2015.

[8] D. A. Pardo, G. E. Jabbour, and N. Peyghambarian, "Application of screen printing in the fabrication of organic light‐emitting devices," *Advanced Materials*, vol. 12, no. 17, pp. 1249-1252, 2000.

[9] S. P. Sreenilayam, I. U. Ahad, V. Nicolosi, and D. Brabazon, "Mxene materials based printed flexible devices for healthcare, biomedical and energy storage applications," *Materials Today*, vol. 43, pp. 99-131, 2021.

[10] M. Sophocleous and J. K. Atkinson, "A review of screen-printed silver/silver chloride (Ag/AgCl) reference electrodes potentially suitable for environmental potentiometric sensors," *Sensors and Actuators A: Physical*, vol. 267, pp. 106-120, 2017.

[11] J. K. Atkinson, M. Glanc, M. Prakorbjanya, M. Sophocleous, R. Sion, and E. Garcia‐Breijo, "Thick film screen printed environmental and chemical sensor array reference electrodes suitable for subterranean and subaqueous deployments," *Microelectronics International*, 2013.

[12] L. Pahlevani, M. R. Mozdianfard, and N. Fallah, "Electrochemical oxidation treatment of offshore produced water using modified Ti/Sb-SnO2 anode by graphene oxide," *Journal of Water Process Engineering*, vol. 35, p. 101204, 2020.

[13] S. Cometa, M. A. Bonifacio, M. Mattioli-Belmonte, L. Sabbatini, and E. De Giglio, "Electrochemical strategies for titanium implant polymeric coatings: The why and how," *Coatings*, vol. 9, no. 4, p. 268, 2019.

[14] S.-J. Potts, C. Phillips, E. Jewell, B. Clifford, Y. C. Lau, and T. Claypole, "High-speed imaging the effect of snap-off distance and squeegee speed on the ink transfer mechanism of screen-printed carbon pastes," *Journal of Coatings Technology and Research*, vol. 17, no. 2, pp. 447-459, 2020.

[15] M. P. Aleksandrova and S. K. Andreev, "Design Methodology and Technological Flow of Screen-Printed Thick-Film Sensors," *IEEE Sensors Journal*, 2021.

[16] F. Hof *et al.*, "Conductive inks of graphitic nanoparticles from a sustainable carbon feedstock," *Carbon*, vol. 111, pp. 142-149, 2017.

[17] J. B. Cook, T. C. Lin, H.-S. Kim, A. Siordia, B. S. Dunn, and S. H. Tolbert, "Suppression of electrochemically driven phase transitions in nanostructured MoS2 pseudocapacitors probed using operando X-ray diffraction," *ACS nano*, vol. 13, no. 2, pp. 1223-1231, 2019.

[18] E. Colín-Orozco, S. Corona-Avendaño, M. Ramírez-Silva, M. Romero-Romo, and M. Palomar-Pardavé, "On the electrochemical oxidation of dopamine, ascorbic acid and uric acid onto a bare carbon paste electrode from a 0.1 M NaCl aqueous solution at pH 7," *Int. J. Electrochem. Sci*, vol. 7, no. 7, pp. 6097-6105, 2012.

[19] M. Kumar, M. Wang, B. K. Swamy, M. Praveen, and W. Zhao, "Poly (alanine)/NaOH/MoS2/MWCNTs modified carbon paste electrode for simultaneous detection of dopamine, ascorbic acid, serotonin and guanine," *Colloids and Surfaces B: Biointerfaces*, vol. 196, p. 111299, 2020.

[20] C. Wang, A. J. Appleby, and F. E. Little, "Charge–discharge stability of graphite anodes for lithium-ion batteries," *Journal of Electroanalytical Chemistry*, vol. 497, no. 1-2, pp. 33-46, 2001.

[21] R. Tatara *et al.*, "The effect of electrode-electrolyte interface on the electrochemical impedance spectra for positive electrode in Li-ion battery," *Journal of The Electrochemical Society*, vol. 166, no. 3, p. A5090, 2018.

[22] E. Barsoukov and J. R. Macdonald, "Impedance Spectroscopy Theory, Experiment, and," *Applications, 2nd ed.(Hoboken, NJ: John Wiley &Sons, Inc., 2005)*, 2005.